Numerical simulation and experimental examination of forming defects in multi-point deep drawing process

B. Beglarzadeh*, B. Davoodi**

*Department of Mechanical Engineering, Science and Research branch, Islamic Azad university, Tehran, Iran, Babak.Beglarzadeh@gmail.com
**School of Mechanical Engineering, Iran University of Science and Technology, Tehran, Iran, bdavoodi@iust.ac.ir

1. Introduction

Forming is a science in which principles and methods of deformation of deformable solids by force are investigated. Metal forming consists of processes in which a metal billet or blank is formed by some tools or die. Multipoint forming is a flexible manufacturing method for 3-d surfaces. Its main idea is a division of the whole die into many mandrels that can be adjusted regularly and accurately. These mandrels constitute "continuous multipoint die". 3-d surfaces can be formed via continuous multipoint die. The multipoint forming concept was first presented in Japan. Nakajima presented adjustable discrete surface die concept for the first time [1]. Nishioka manufactured Universal pressure test kit which was indeed an adjustable separate die [2]. The universal pressure test kit is comprised of upper and lower flexible dies controlled by computer. Walzik carried out extensive research regarding multipoint forming in the United States. They offered the closed-loop control system for continuous die of discrete pieces and manufactured test equipments controlled by computer [3]. Finkschtian in Germany controlled flexibility developments and tool system for deep drawing and stretch numerically. They referred to a tool system which includes a matrix comprising 1089 rods and stretch die was formed by adjusting them separately [4]. Rao in India provided a continuous surface in tools, discrete surface with a flexible sheet like rubber materials and called it a flexible surface tool. Computational simulation was carried out on the flexible surface and revealed that optional flexible surface for sheet forming process in general and for such processes as composite layers in specific [5]. Li studied the basic theory and practical technology of multipoint forming in China. For basic theory, they offered four main methods for multipoint forming and replicated forming method that can control effectively the bouncy return [6]. He also offered a new method named as continuous multipoint forming, which is a combination of multipoint forming and continuous forming (rolling). They have developed experimental equipments and have carried out some experiments. The experiment results reveal that 3-d surface can be formed by the continuous forming method [7]. Wong investigated principles and development of spinning. They depicted that pinning has a potential in the development of complicated forms manufacturing, which is required in the increased number of productions by global industries [8]. Music studies, the most practical work in analyzing and using spinning mechanics. They demonstrated that the existing work represents multiple gaps in the current science of spinning mechanics, and studying spinning process features reflects that there is a great potential for innovation in spinning [9]. Wrinkle and rupture is the most common defects created in this process, similar to ordinary deep drawing method. Indentation of the sheet due to direct contact with the tip of the pin with sheet surface is another defect which may be created during metal sheet formation by the multipoint forming process. In the following, the above mentioned defects are introduced and parameters effective on these defects will be investigated. Fig. 1 schematically shows the procedures of Multipoint forming.
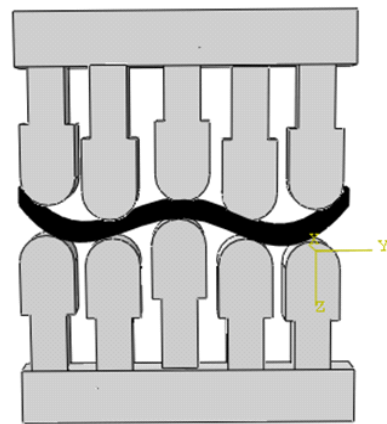

Fig. 1 Schematic diagram of Multi-point forming

2. Literature review

2.1. Theoretical principles

2.1.1. Deep drawing process

Deep drawing is the most common method of shell piece forming. Due to producing various pieces with high quality and speed and low costs, this method has been increasingly applied. In this process, many parameters such as friction, drawing ratio, quality and type of die and sheet, blank holder force, drawing speed, mandrel head radius, and matrix edge is involved. Deep drawing is cold forming and plastic deformation occurs without material removal. In the deep drawing process, there are four separate areas and deformation mechanics of one area differs from another one.

2.1.2. Multi-point forming process

Among sheets formation methods, new formation methods that use flexible die and do not need multiple rigid dies, have recently drawn the attention of researchers. Multi-point formation is a flexible technique to produce metal sheets with 3-d geometry. In multi-point formation

process, the pins have been designed in a way that are independent from each other and are adjusted easily. So, controlling pin height may create a continuous working surface. In multi-point formation, curved surface of the die has been created by a large number of pins. In this method, independent pins are used instead of traditional dies .

3. Research tools and materials

Here, equipments applied in the test and geometrical features of final work-piece will be introduced. Then different stages, die components, sample preparation, used materials, and the manner of obtaining mechanical features will be elaborated.

3.1. Equipments

To implement experiments, a dual-purpose hydraulic press T.S.S. with a capacity of 200 KN has been applied.

3.1.1. Multipoint forming die

To manufacture this die, 300 hemispherical head pins have been applied. These pins are independent from

each other and have been designed in a way that their heights are easily adjustable. So adjusting pin height properly may create surfaces with different curvatures. The blank holder force required in the forming process is supplied by the lower jack of the press kit. Geometrical dimensions of the rigid die are shown in Table 1. a polyurethane layer with a Shore A is used. Thickness of the Al2024 sheet is 1 mm.

Table 1

Geometrical dimensions of the rigid die

Parameter	Size, mm
Pin diameter	14
Die enterance radius	9
Matrix hole dimension	230 × 230
Sheet dimension	300 × 300
Polyurethane layer thickness	12

3.1.2. Mechanical features of polyurethane layer and sheet

The tested material is 2024 aluminum alloy with a thickness of 1 mm. The chemical composition of this alloy is presented in Table 2.

Table 2

Chemical composition of 2024 aluminum alloy

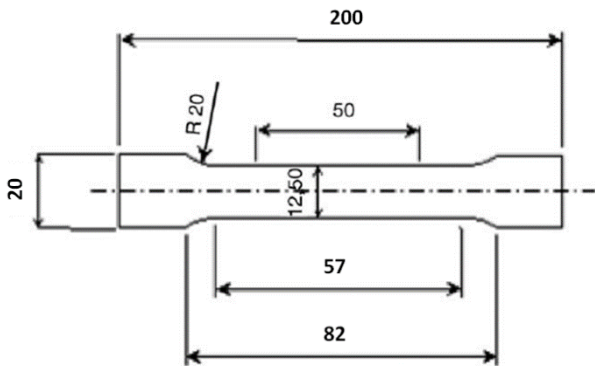| Material	Si%	Fe%	Cu%	Mn%	Mg%	Cr%	Zn%	Ti%
AA2024	0.50	0.50	4.3- 4.5	0.5- 0.6	1.3-1.5	0.10	0.25	0.15

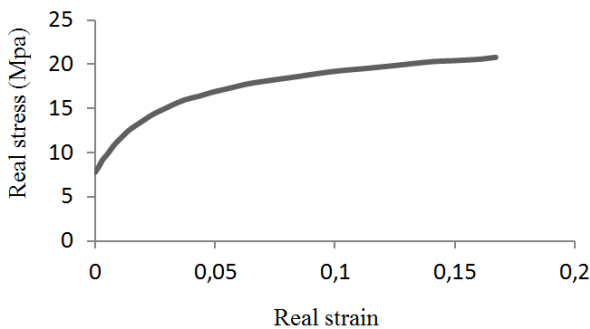Fig. 2 The sample used for simple stretch test

Fig. 3 Real stress – strain diagram of 2024 aluminum alloy

To obtain mechanical features of the samples, uniaxial stretch test has been applied. In so doing, as shown in Fig. 2, samples of 2024 aluminum alloy are prepared based on ASTM B557m and with a basic length of 50 mm and

width of 12.5 mm. To obtain such features as yield strength, final strength, and the stress-strain diagram, the standard sample was prepared in the rolling direction and was drawn by the puller to reach fracture.

Having implemented the uniaxial stretch test, the real stress-strain diagram related to 2024 aluminum alloy is obtained as per Fig. 3.

Thickness strain is usually obtained by measuring longitudinal and transverse strains and using the principle of constant volume as per $\varepsilon_t = \left(\varepsilon_w + \varepsilon_l \right)$. To obtain anisotropy coefficient, samples are prepared in the rolling direction which makes a 45 degree angle with the rolling direction and in a direction perpendicular to the rolling and are put under uniaxial stretch, and longitudinal and transverse strains of all three samples are measured. Then anisotropy coefficient is obtained by below relation:

$$R = \frac{d\varepsilon_w}{d\varepsilon_t} = -\frac{d\varepsilon_w}{d\varepsilon_l + d\varepsilon_w} = -\frac{\varepsilon_w}{\varepsilon_l + \varepsilon_w}.$$

With regard to the above relation, anisotropy coefficient values of 2024 aluminum alloy are presented in Table 3.

Table 3

Anisotropy coefficient values of 2024 aluminum alloy in different directions

Alloy	R_0	R_{45}	R_{90}	$\bar{R}$
2024 Aluminum	0.73	0.75	0.77	0.75

In Table 2, $\bar{R}$ is obtained through below relation:

$$\bar{R} = \frac{1}{4}\left(R_0 + 2R_{45} + R_{90}\right) . 0°.$$

The mechanical properties are presented in Table 4.

Table 4

Mechanical properties of AA2024-O aluminum alloy

Sheet direction relative to rolling direction	Yield strength, MPa	Modulus of elasticit, GPa	Strain hardening, n	Strength, MPa	Anisotropy, R
0°	79	73	0.2662	353.08	0.73
45°	76	73	0.2565	353.02	0.75
90°	77	73	0.2427	338.04	0.77

One of the most common defects that can occur in the formed parts using multi point deep drawing method is dimple which depends on the nature of the process itself and it causes when pins are in direct contact with the surface of the sheet.In order to prevent the creation of dimples, flexible material (polyurethane) is used between the plate and the pin. To determine properties of polyurethane applied in this paper, the standard test (ASTM D575-91) has been used. According to this standard, sample have a cylindrical shape with a diameter of 27.6 mm and a height of 5.12 mm to be prepared and impact speed 12 mm per minute stay on under pressure tests.Fig. 4 shows a polyurethane sample image which is preparing for the pressure test.
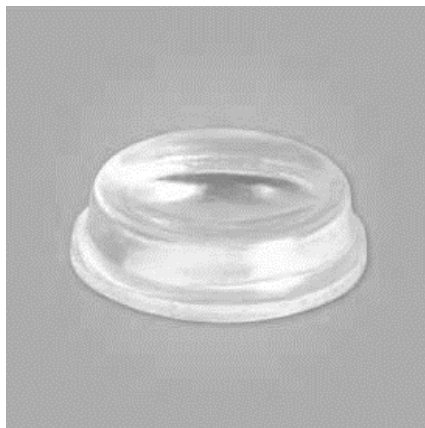

Fig. 4 Prepared polyurethane sample for testing pressure

4. Finite elements simulation

In this study, ABAQUS/EXPLICIT 6.14.1 software is used for simulation, to determine whether the shrinkage of the part and Also considers the effects of anisotropy in sheets of aluminum, three-dimensional models have been used to analyze. Also, due to the symmetry and reduced the analysis time only a quarter of the mold and the plate is modeled. Sheet mode of the shell and deformable, elastic layer of solid and definable, pin, matrix and blankholder of discrete rigid is determined. Since mold components, including pins, blank-holder and matrix are modeled as rigid surfaces, mechanical properties is not attributed to them. Simulations of the used process have been set in two-step. In the first step, the blank-holder force is applied to the upper surface of the plate, and the second step is to move the upper punches to create the desired shape.

Contact between the sheet surfaces with polyurethane layer and the mold surfaces are selected surface to surface type. Blank-holder surface 0.1, is considered. This coefficient for the contact surface between the sheets and a layer of polyurethane, and polyurethane layer to the surface of the pins are 0.1 and 0.2, respectively. Elements used in the model of plate are S4R. In order to model the friction of the interface of plate surfaces with die components surfaces and polyurethane layer, the Coulomb friction model is used. According to reference [10] the friction coefficient between the sheet contact surface with mold
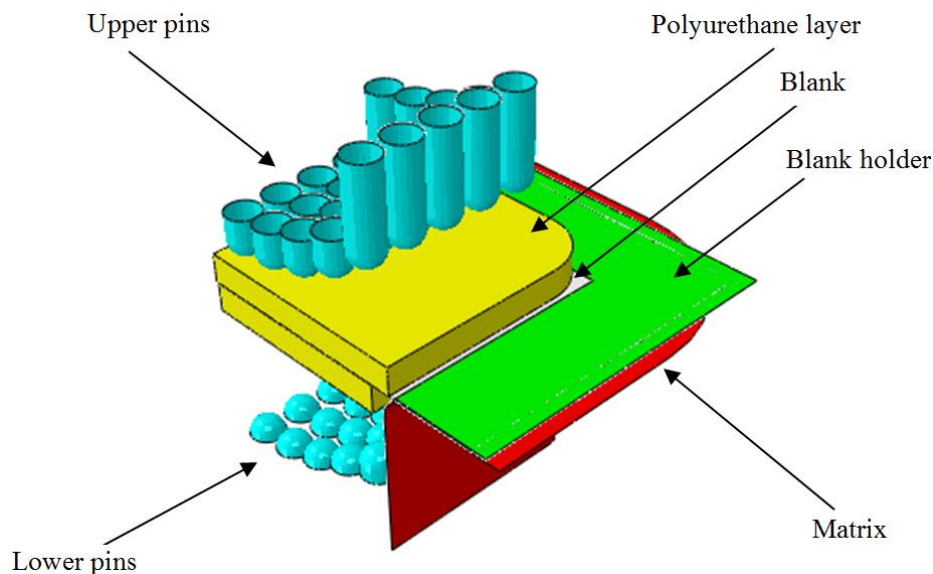

Fig. 5 The assembly of mold component and sheet in simulation

and four-node element. For meshing the layers of polyurethane, the eight-node solid element C3D8R is used. And elements used in the upper and lower matrix, pins and components of the die are R3D4. For investigation of the grain size effect, thickness changes at critical points of the work piece and also the time of the analysis process in various scenarios comparing and at the end with probing the results, 0.0015 for numeric grading is selected. Assembly of mold component is shown in Fig. 5.

4.1. Fracture prediction in finite element simulation

To investigate the effect of the yield criterion on the formed sheet rupture, Hill's 1948 yield criterion with below formula has been applied:

$$2f = F\left(\sigma_y - \sigma_z\right)^2 + G\left(\sigma_z - \sigma_x\right)^2 +$$
$$+H\left(\sigma_x - \sigma_y\right)^2 + 2L\tau_{yz}^2 + 2M\tau_{zx}^2 + 2N\tau_{yx}^2. \quad (1)$$

For isotropic plate state, the formula is as below:

$$\sigma_1^2 + \sigma_2^2 + r\left(\sigma_1 + \sigma_2\right)^2 = (1+r)\sigma_u^2. \quad (2)$$

In the above relation, σ_u denotes yield stress in uniaxial strain, r represents anisotropy coefficient, and σ_1 and σ_2 are main stresses. With regard to the relation (2), below relation is established for greater anisotropy coefficients.

$$\sigma_b = \sqrt{\frac{r+1}{2}}\sigma_u. \quad (3)$$

In the above relation, σ_b denotes yield stress in biaxial strain. Relation (3) indicates that for the anisotropy coefficients greater than one, yield stress of uniaxial strain must be smaller than the yield stress of biaxial strain, and vice versa.

During recent years, many soft fracture criteria have been offered some of which are based on a defect growth ratio presented by Rice and Tracey. One of them is Cockcroft-Latham criterion which is based on total plastic work per unit volume. They stated fracture criterion on the basis of real formation by which fracture occurs in soft materials when below conditions is provided.

$$\int_0^{\bar{\varepsilon}_f} \sigma_{max} d\bar{\varepsilon} = C_1. \quad (4)$$

In the above relation, σ_{max} denotes maximum tensile stress, ε_f is the equivalent strain at which rupture occurs, and C_1 represents the constant related to the type of material. This paper applies Clift and Cockcroft-Latham criteria. To determine the constant of ductile fracture criterion depending upon the number of criterion constants, uniaxial strain test, Plane strain tests, or Bulge test is applied. If the criterion has one constant, uniaxial strain test is only applied; and if there are more constants, plane strain test or Bulge test is used. Since this paper has used Clift and Cockcroft-Latham criteria which have one constant, uniaxial strain test is applied to obtain their constant.

5. Results and discussions

Here, the results obtained from experiments and simulations are presented. Defects which is created during the multi point deep drawing process, are investigated.

5.1. Defects studied in this paper

Wrinkle and rupture is the most common defects created in this process, similar to ordinary deep drawing method. Indentation of the sheet due to direct contact with the surface of the pin with sheet surface is another defect which may be created during metal sheet formation by the multipoint forming process. In the following, the above mentioned defects are introduced and parameters effective on these defects will be investigated.

5.1.1. Wrinkle

During the formation of complicated 3-d pieces with high deformation, compressive stresses are created on the plate that lead frequently to damage due to wrinkles. To remove wrinkles, blank holder force may be used in multipoint forming process. The pieces formed under different blank holder forces were tested through using finite element simulation. The polyurethane layer with thickness of 10 mm and hardness of 65 SA was applied to experiments. Samples formed in the experimental tests and simulation by using blank holder forces of 1200, 1600, and 2000 Newton is depicted in Fig. 6.

As shown in the above figure, by increasing blank holder force up to 2000 Newton, wrinkles are gradually reduced and ultimately by exerting blank holder force of 2000 Newton, a perfect piece may be formed. As blank holder force increases, wrinkles are reduced.

5.1.2. Rupture

If a piece is put under an increasing load, it will fracture. This fracture may be brittle or coupled with plastic deformation and it is primarily soft. In ductile fracture, the required plastic deformation is restricted to the specific states up to fracture stage. That is, little energy is consumed. So from an engineering perspective, this is a brittle fracture. This state can be observed in sharp lines and cracks under a relatively low nominal stress; particularly in the plain strain state that reduces plastic deformation probability. The most common soft fracture occurs in an organ with tensile loading under too much load whose fracture is conical (necking and breaking). When the load reaches maximum amount, plastic strain becomes non-uniform and focuses on a small part of the organ and necking occurs. If tensile loads are too much severe, sheet thickness reduces and then it is ruptured. Corner rupture may reach even flat wall of the cube. Fig. 7 depicts how wrinkles and rupture are created in the corner.
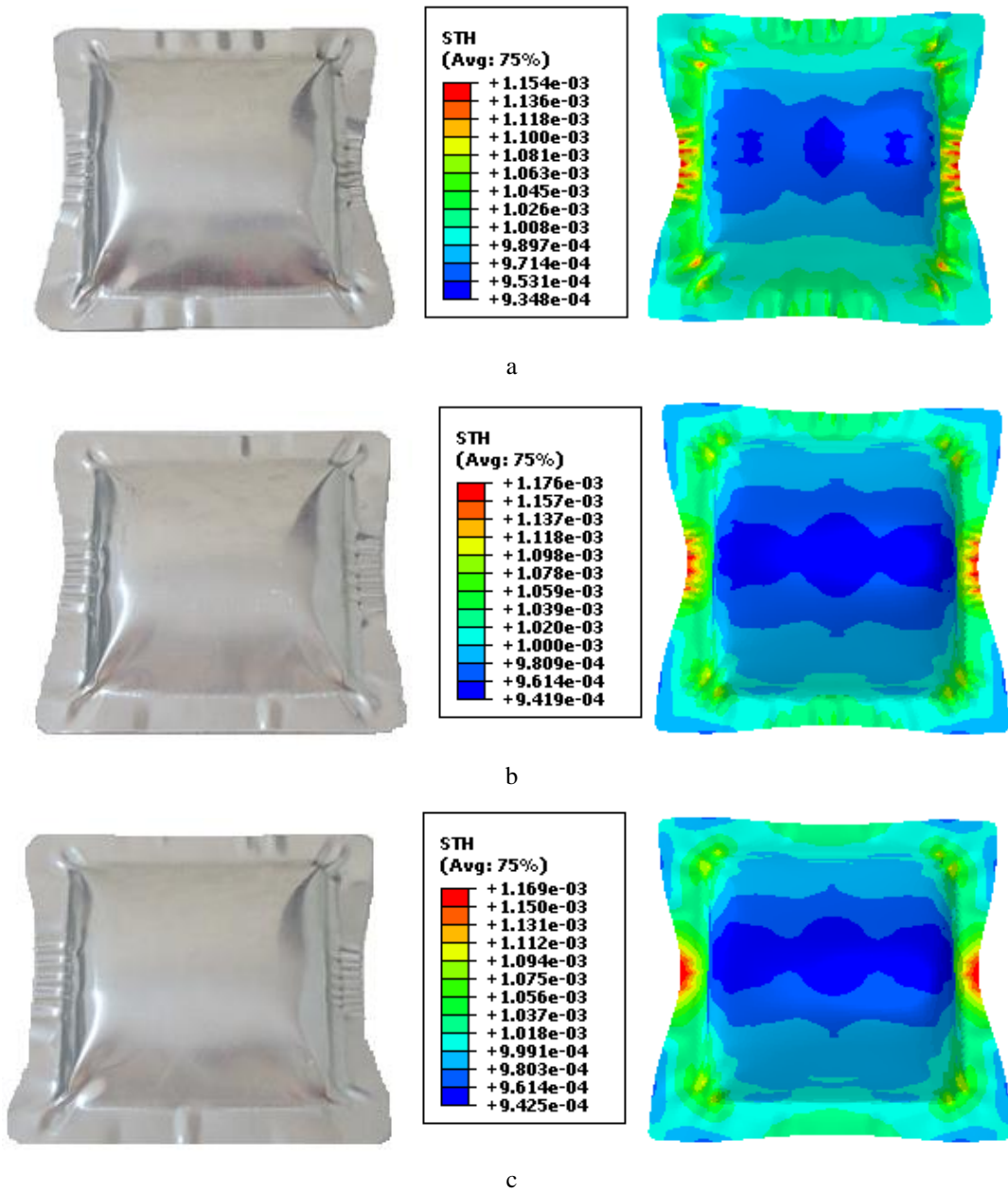
a

b

c

Fig. 6 Blank holder force of: a - 1200 Newtons; b - 1600 Newton; c - 2000 Newton
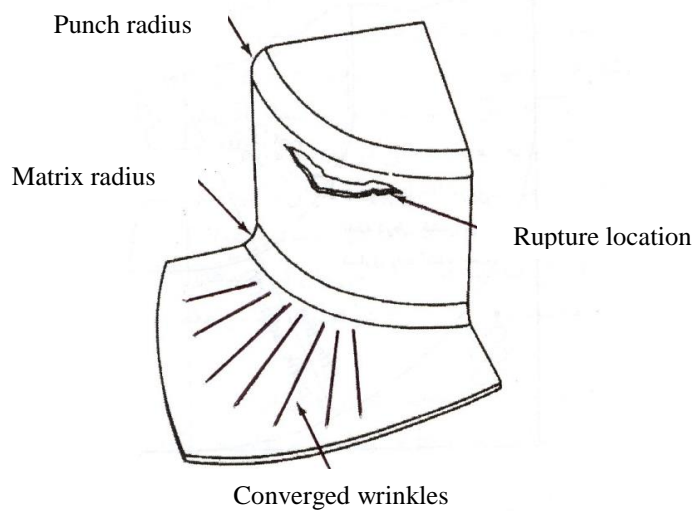

Fig. 7 Strain analysis in corners

Through using stresses and strains obtained by simulation and constants of the material presented in Table 5, relations (5) and (6) are calculated for each element. The above relations, satisfaction occurs when the integral value reaches one. When the integral value equals one, the element has been ruptured. First, we investigate a simulated model of Fig. 8 by using two Cockcroft-Latham and Clift criteria [11].

Table 5

Material constants for each criterion

Soft fracture criterion	Material constant
Cockcroft-Latham	30.587
Clift	29.987

Cockcroft and Latham:

$$\int_0^{\bar{\varepsilon}_f} \sigma_{max} d\bar{\varepsilon} = C_1 ; \tag{5}$$

Clift et al.:

$$\int_0^{\bar{\varepsilon}_f} \bar{\sigma} d\bar{\varepsilon} = C_2 , \tag{6}$$

where σ_{max} is the maximum principle stress, $\bar{\varepsilon}$ is the equivalent strain, $\bar{\varepsilon}_f$ is the equivalent strain at which the fracture occurs, C_1 is the material constant to express the limit of ductile damage. The integral showing in Eqs. (7) and (8) is the normalized damage value of Eq. (5) and (6).This integral is calculated at each integration points (Gauss points), using the stresses and strains computed by finite element analysis. If the integral at Gauss point of an element becomes 1, its damage value in the element reaches the fracture criterion and element is deleted.

$$I_1 = \frac{1}{C_1} \int_0^{\bar{\varepsilon}} \sigma_{max} d\bar{\varepsilon} ; \tag{7}$$

$$I_2 = \frac{1}{C_2} \int_0^{\bar{\varepsilon}} \bar{\sigma} d\bar{\varepsilon} . \tag{8}$$

Fig. 8 shows the simulation model to calculate the integral I. In this section, for each of the elements that are located in a critical region, the integral Ij is calculated with using of the Cockcroft - Latham and Clift criteria.

Here, we calculate integral I for each element located at the critical zone by using Cockcroft-Latham and Clift criteria. Table 6 presents the numbers related to each criterion.

Table 6

Criteria calculated for each element

Element No.	Cockcroft-Latham Criterion (I_1)	Clift criterion (I_2)
1	0.946	0.957
2	0.921	0.931
3	1.249	1.263
4	0.899	0.909
5	0.857	0.866
6	0.797	0.806
7	1.147	1.159
8	0.931	0.941
9	1.194	1.208

Comparison of numbers related to each element reflects that the elements of Clift criterion reach rupture earlier. As the value of elements No. 3, 7, and 9 have reached one, they are ruptured. Other elements are not ruptured as their value has not reached one.

In this section, by doing experimental tests under different conditions, as well as finite element simulation, it can be seen that the results are in good agreement. These results are given in the Fig. 9.

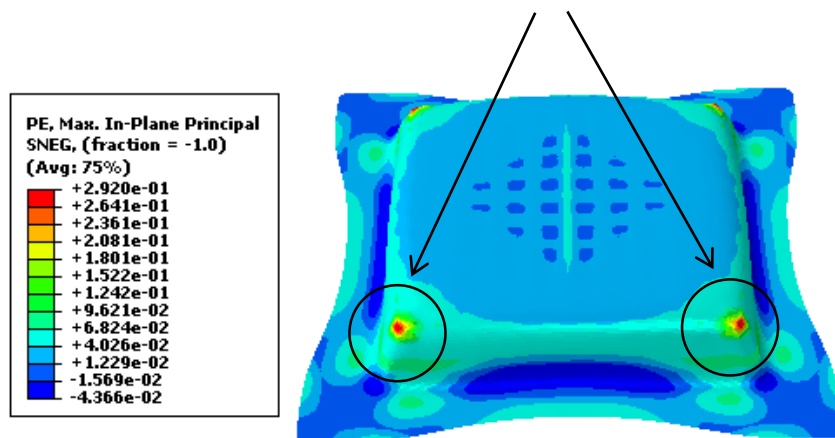Investigation of rupture zones by using ductile fracture

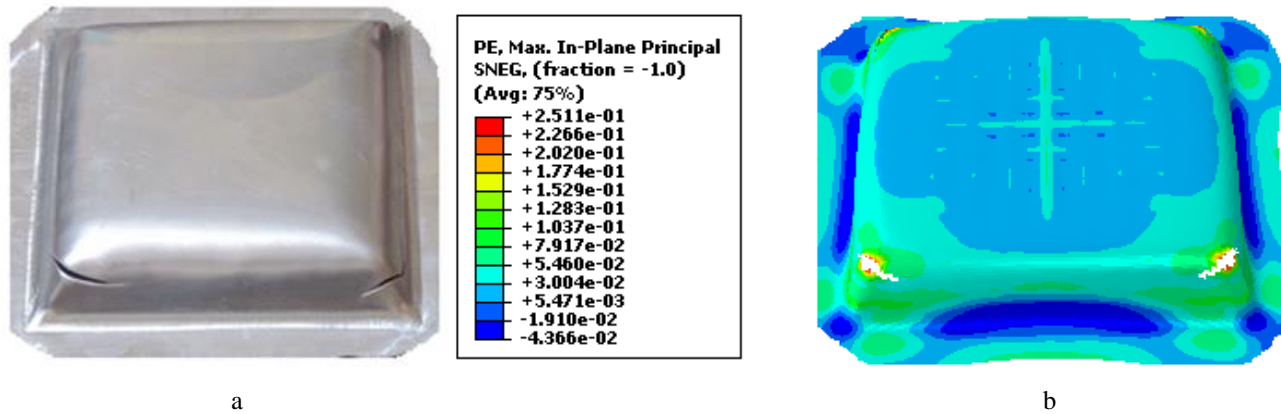Fig. 8 The model simulated for calculating the integral I

a   b

Fig. 9 Torn samples that has done by polyurethane with a hardness of 80 S.A and thickness of 12 mm: a – experimental; b - simulation

6. Conclusion

- According to the results, as the blank holder force increases up to 2000 Newton, folds were removed gradually and finally a perfect piece may be formed by exerting 2000 Newton blank holder force.

- Comparison of Cockcroft-Latham and Clift criteria of each element indicates that elements pertaining to Clift criterion are ruptured earlier.

References

1. **Nakajima, N.** 1969. Research on die and electrode by steel wire bind, Japanese Journal of Mechanical Academy 72: 32-40.

2. **Nishioka, F.** 1973. An automatic bending of plates by the universal press with multiple piston heads (Second report: practicality researcher), Journal of the Society of Naval Architects of Japan 133: 291-305. http://dx.doi.org/10.2534/jjasnaoe1968.1973.291.

3. **Walczyk, D.F.; Hardt, D.E.** 1998. Design and analysis of reconfigurable discrete dies for sheet metal forming, Journal of Engineering for Industry 6: 436-454. http://dx.doi.org/10.1016/s0278-6125(99)80003-x.

4. **Finckenstein, E.V.; Kleiner, M.** 1991. Flexible numerically controlled tool system for hydro-mechanical deep drawing, CIRP-Manufacturing Technology 40: 311-314. http://dx.doi.org/10.1016/S0007-8506(07)61994-5.

5. **Rao, P.V.M.; Dhande, S.G.** 2002. A flexible surface tooling for sheet-forming processes conceptual studies and numerical simulation, Journal of Materials Processing Technology 124: 133-143. http://dx.doi.org/10.1016/S0924-0136(02)00141-3.

6. **Li, M.; Liu, Y.; Su, Sh.; Li, G.** 1999. Multi point forming: a flexible manufacturing method for 3-d surface sheet, Journal of material processing technology, 277-280. http://dx.doi.org/10.1016/S0924-0136(98)00364-1.

7. **Li, M.Z.; Cai, Z.Y.; Sui, Z.; Yan, Q.G.** 2002. Multi point forming for sheet metals, 333-338.

8. **Wong, C.C.; Dean, T.A.; Lin, J.** 2003. A review of spinning, shear forming and flow forming processes, Journal of Machine Tools and Manufacture 43: 1419-1435. http://dx.doi.org/10.1016/S0890-6955(03)00172-X.

9. **Music, O.; Allwood, J.M.; Kawai, K.** 2010. A review of the mechanics of metal spinning, Journal of Materials Processing Technology 210: 3-23. http://dx.doi.org/10.1016/j.jmatprotec.2009.08.021.

10. **Yanxiong Liu; Lin Hua** 2010. Fabrication of metallic bipolar plate for proton exchange membrane fuel cells by rubber pad forming, Journal of Power Sources 195: 3529-3535. http://dx.doi.org/10.1016/j.jpowsour.2009.12.046.

11. **Takuda, H.; Morib, K.; Hatta, N.** 1999. The application of some criteria for ductile fracture to the prediction of the forming limit of sheet metals, Journal of Materials Processing Technology 95: 116-121. http://dx.doi.org/10.1016/S0924-0136(99)00275-7.

12. **Ghajar, Rahmatollah** 2009. Mechanics of Fracture and Fatigue, School of Mechanical Engineering, K. N. Toosi University of Technology, Publication of K. N. Toosi University of Technology.

13. **Hasford, Wiliam; Kedel, Robert** 2009. Metal forming (Metallurgy and Mechanics), translated by Mohammad Reza Afzali, Tehran: Sharif University of Technology, Elmi Publication.

14. **Johnson, W.; Melur, P.** 1999. Engineering Plasticity, translated by Dr. Karen Abarinia, Tehran: Ya Mahdi Industrial Group, Ya Mahdi Publication.

15. **Li, M.Z.; Cai, Z.Y.; Sui, Z.; Yan, Q.G.** 2002. Multi point forming technology for sheet metals, J. Mater. Proc. Technol. 129: 333-338. http://dx.doi.org/10.1016/S0924-0136(02)00685-4.

16. **Sun, G.; Li, M.Z.; Yan, X.P.; Zhong, P.P.** 2007. Study of blank-holder technology on multi-point forming of thin sheet metal, J. Mater. Proc. Technol. 187-188: 517–520. http://dx.doi.org/10.1016/j.jmatprotec.2006.11.133.

17. **Tan, F.X.; Li, M.Z.; Cai, Z.Y.** 2007. Research on the process of multi-point forming for the customized titanium alloy cranial prosthesis, J. Mater. Proc. Technol. 187-188: 453-457. http://dx.doi.org/10.1016/j.jmatprotec.2006.11.149.

18. **Tarkesh, Esfahani, Rasoul; Gharaei, Amin; Shah Nazari, Hossein; Nejatbakhsh, Hasan** 2011. Comprehensive guide to modeling and analysis in ABAQUS software, Abed Publication.

19. **Xue-peng Gong; Ming-zhe Li; Qi-peng Lu; Zhong-qi Peng** 2012. Research on continuous multi-point forming

method for rotary surface, Journal of Materials Processing Technology 212: 227-236.
http://dx.doi.org/10.1016/j.jmatprotec.2011.09.008.

20. **Zareh, B.; Vafaeesefat, A.; Rikhtegar-Nezami, V**.
2013. Experimental and numerical investigation of sheet metal forming using multi-point forming process, Aerospace Mechanics Journal 8(4): 87-75.

B. Beglarzadeh, B. Davoodi

NUMERICAL SIMULATION AND EXPERIMENTAL
EXAMINATION OF FORMING DEFECTS IN
MULTI-POINT DEEP DRAWING PROCESS

S u m m a r y

Significant reductions in manufacturing costs are required to make structural material attractive for mass production applications such as automotive components. This can be achieved through highly efficient multi point forming operation, which has proven its ability to produce metal products with very good structural integrity and quality. This paper aims at studying forming defects which occur in multi-point deep drawing method through simulation and experimentation. In this study, commercially available finite element software ABAQUS / EXPLICIT 6.14.1 was used for the simulation of forming procedure. In order to analyze sheet behavior in multi point deep drawing procedure and also representing defects which may happen during the forming process, three-dimensional models will be utilized. The experimental tests were carried out through using Sheets of aluminum alloy 2024 with an initial size of 300×300 mm. Defects created in the multi-point forming process was investigated and rupture of forming sheet was predicted by using ductile fracture criteria. Studying blank holder force for Polyurethane layers with different hardness reveals that blank holder force increase has a direct relation with the increase in polyurethane layer hardness. The results of simulation depict that by increase in the thickness of polyurethane layer, the rate of indentation is reduced. By comparison of the Cockcroft – Latham and Clift criteria of each element, it is seen that elements which are related to Clift criterion reach to rupture earlier.